Article

Photoinduced *meta*-Selective C−H Oxygenation of Arenes

Wajid Ali,[⊥] Argha Saha,[⊥] Haibo Ge,* and Debabrata Maiti*

Read Online

ACCESS | Metrics & More | Article Recommendations | Supporting Information

ABSTRACT: The merger of photocatalysis and transition-metal catalysis has recently emerged as an adaptable platform for the development of innovative and environmentally benign synthetic methodologies. In contrast to classical transformation by Pd complexes, photoredox Pd catalysis operates through a radical pathway in the absence of a radical initiator. Using the synergistic merger of photoredox and Pd catalysis, we have developed a highly efficient, regioselective, and general *meta*-oxygenation protocol for diverse arenes under mild reaction conditions. The protocol showcases the *meta*-oxygenation of phenylacetic acids and biphenyl carboxylic acids/alcohols and is also amenable for a series of sulfonyls and phosphonyl-tethered arenes, irrespective of the nature and position of the substituents. Unlike thermal C−H acetylation which operates through the Pd^{II}/Pd^{IV} catalytic cycle, this metallaphotocatalytic C−H activation involves Pd^{II}/Pd^{III}/Pd^{IV} intermediacy. The radical nature of the protocol is established through radical quenching experiments and EPR analysis of the reaction mixture. Furthermore, the catalytic path of this photoinduced transformation is established through control reactions, absorption spectroscopy, luminescence quenching, and kinetic studies.

KEYWORDS: *distal C, H activation, Pd-photoredox catalysis, phenylacetic acid drugs, acetoxylation, radical mechanism*
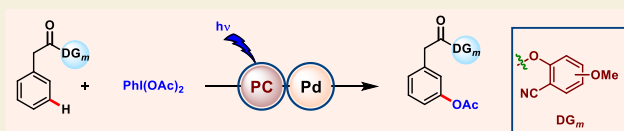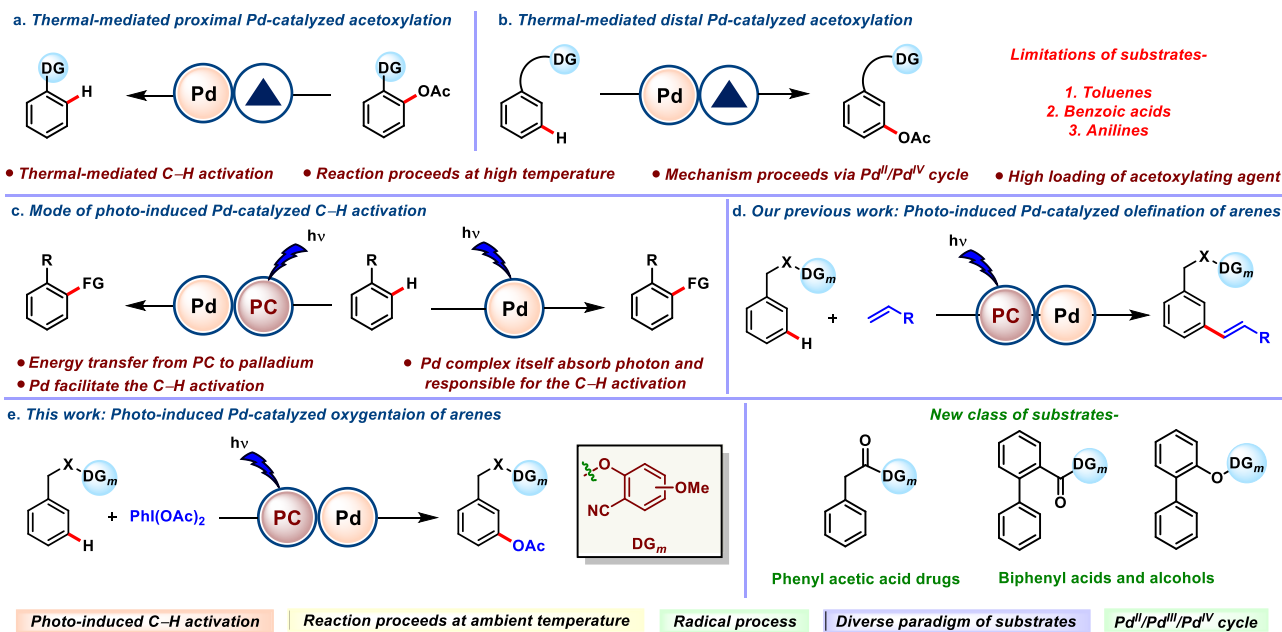
In recent years, transition-metal-catalyzed C−H bond functionalization gains tremendous expansion due to the easy accessibility of C−H bonds in various molecular systems.[1−5] Among several C−H functionalization reactions, the construction of the C−O bond attracted much attention in organic synthesis due to its ability to induce polar nature and a unique H-bond donor-accepting capacity. In particular, the installation of the acetoxy group enhances antimicrobial and herbicidal activities in many molecules and is also found in many marketed drugs and natural products.[6−11] As a consequence, a number of acetoxylation reactions ranging from proximal to distal C(sp^2)−H bonds were developed (Scheme 1a,b).[12−25] However, most of these protocols suffer from pitfalls such as the use of excess acetoxylating reagent, high temperature, and use of acids (acetic acid or acetic anhydride) as additives or solvents, which limit their application in the substrates bearing sensitive functional groups and complex moieties. Furthermore, distal C(sp^2)−H acetoxylation reactions are limited to the substrates with toluene, benzoic acid, and aniline backbones (Scheme 1b). To overcome these limitations, a sustainable protocol is required, which operates under milder conditions and avoids superstoichiometric amounts of acetoxylating reagents and is applicable for the substrates which are unexplored under thermal conditions. The recent resurgence in photochemistry has aided the development of numerous transformations in the arena of organic chemistry which were previously inaccessible.[26−43] Very recently, a unique class of photocatalysis termed "photoredox catalysis" has gained momentum and has

been applied by the organic chemistry community worldwide. Photoredox catalysis upon merger with a transition metal (Ni, Pd, Cu, Co, and Au) has led to the accomplishment of prior elusive transformations and received broad attention from organic chemists.[31,44−55] To be precise, the ability of a Pd-catalyzed photoredox reaction to reroute the reaction mechanism via alternative Pd/radical-mediated pathways led to improvement in the reaction rate, substrate scope, and functional group compatibility.[47,51,56,57] In general, Pd-photo-catalyzed reactions work in two different ways (Scheme 1c). The first one is the synergetic cooperativity between a Pd catalyst and a photosensitizer, where an external photocatalyst is a sole light-absorbing species (Scheme 1c, left) and recently gained substantial attention to functionalize a plethora of C−H bonds under ambient conditions.[26,44,51,58−68] In the second mode of reaction, the Pd catalyst itself absorbs the photon energy and catalyzes the reaction via a traditional or new type of mechanism without the requirement of an exogenous photocatalyst (Scheme 1c, right).[52,69−72] This dual activity of Pd was well documented in the literature by various transformations.[73−76] This catalytic transformation usually

Scheme 1. Realm of Pd-Catalyzed Proximal and Distal C−H Activation Reactions

a. *Thermal-mediated proximal Pd-catalyzed acetoxylation*

b. *Thermal-mediated distal Pd-catalyzed acetoxylation*

Limitations of substrates-
1. *Toluenes*
2. *Benzoic acids*
3. *Anilines*

- *Thermal-mediated C−H activation*
- *Reaction proceeds at high temperature*
- *Mechanism proceeds via Pd^{II}/Pd^{IV} cycle*
- *High loading of acetoxylating agent*

c. *Mode of photo-induced Pd-catalyzed C−H activation*

- *Energy transfer from PC to palladium*
- *Pd facilitate the C−H activation*
- *Pd complex itself absorb photon and responsible for the C−H activation*

d. *Our previous work: Photo-induced Pd-catalyzed olefination of arenes*

e. *This work: Photo-induced Pd-catalyzed oxygentaion of arenes*

New class of substrates-

Phenyl acetic acid drugs   *Biphenyl acids and alcohols*

Photo-induced C−H activation | *Reaction proceeds at ambient temperature* | *Radical process* | *Diverse paradigm of substrates* | *Pd^{II}/Pd^{III}/Pd^{IV} cycle*

follows a single catalytic cycle in contrast to photoredox catalysis.[77]

Converging this alluring property of Pd catalysis and photocatalysis, recently, our group reported a highly regioselective $C(sp^2)$−H olefination of arenes and hetero-arenes, including distal $C(sp^2)$−H olefination through the directing group assistance (Scheme 1d).[78] Inspired by our earlier success, herein, we demonstrated photoredox Pd catalysis for the *meta*-oxygenation of arenes (Scheme 1e). This synergetic effect of photoredox and Pd catalysis aids to perceive a new class of substrates like phenyl acetic acids, biaryl acids, and alcohols which are not reported earlier. To demonstrate the superiority of our protocol over thermal conditions, parallel experiments under thermal conditions (at 80 °C) were performed, and results are tabulated in the Supporting Information (see Section 11 and Table S8). Notably, the present catalytic system obviates the use of elevated temperature and a superstoichiometric acetylating agent, which is known to play a pivotal role in the reaction under thermal conditions, and afforded superior selectivity.

We commenced our study with the *meta*-acetoxylation of the phenylacetic acid-bearing nitrile-based template under Pd-photoredox catalysis. To start with our hypothesis, we have taken phenylacetic acids as model substrates, as these variants of acids are well abundant in commercially available drugs. The *meta*-acetoxylation of phenylacetic acids is yet to be explored, either in thermal or photochemical conditions. Here, we report the *meta*-acetoxylation of phenylacetic acids under photoredox conditions. Taking the idea from our previous report, we performed sequential optimization of each reaction parameter (see Supporting Information, Section 3) and found that the use of Pd(OAc)$_2$ (10 mol %), *N*-Cbz-Gly-OH (20 mol %), eosin Y (3 mol %), and visible light (23 W) in HFIP solvent at ambient temperature for 36 h provided the highest yield of 79% of the *meta*-acetoxylated product, with selectivity >25:1 (Table 1, entry 1). Experimentation with diverse directing auxiliaries for the *meta*-functionalization suggests that only a nitrile-based directing template is compatible and also that the

Table 1. Optimization of Photoinduced *meta*-Selective C−H Oxygenation of Arenes

| entry	deviation from standard conditions	yield (%)[a]	selectivity
1	none	79	>25:1
2	no Pd(OAc)$_2$	NR	
3	no light	NR	
4	no eosin Y	NR	
5	Pd(TFA)$_2$ instead of Pd(OAc)$_2$	32	>25:1
6	PdCl$_2$ instead of Pd(OAc)$_2$	trace	
7	Pd(PPh$_3$)$_4$ instead of Pd(OAc)$_2$	NR	
8	Pd(OAc)$_2$ (20 mol %)	71	>25:1
9	fluorescein instead of eosin Y	47	>25:1
10	rhodamin B instead of eosin Y	trace	
11	*N*-Ac-Gly-OH instead of CBz-Gly-OH	41	16:1
12	Fmoc-Gly-OH instead of CBz-Gly-OH	40	17:1
13	*N*-Ac-4-hyrdoxy-L-proline instead of CBz-Gly-OH	21	3:1
14	CBz-Gly-OH (10 mol %)	58	18:1
15	2-hydroxy pyridine instead of CBz-Gly-OH	18	2:1
16	DCE instead of HFIP	NR	
17	TFE instead of HFIP	14	20:1

[a]Yield determined by ^{1}HNMR using TMB (trimethoxy benzene) as the internal standard. Yield given is the sum of the isomers.

methoxy group-bearing template (at the *para* or *meta* position) provides the best yield and selectivity (see Supporting Information, Section 3 and Table S1). To testify the role of Pd catalyst, light, and the photocatalyst in this *meta*-$C(sp^2)$−H acetoxylation reaction, parallel reactions were investigated in the absence of these components (Table 1, entries 2−4). Complete inhibition of the reaction justifies the role of the Pd catalyst, light, and the photocatalyst in endorsing the transformation. Furthermore, Pd catalysts other than Pd-

(OAc)$_2$ were found to be inferior (Table 1, entries 5−8). Photocatalysts other than eosin Y provide lower yields (Table 1, entries 9 and10). Among the different N-protected amino acids and 2-hydroxy pyridine tested, N-Cbz-Gly-OH emerged to be the best (Table 1, entries 11−15). Solvents other than HFIP were found to be ineffective or less productive for this transformation (Table 1, entries 16 and 17). Finally, after a series of optimization, it was established that a catalytic Pd(OAc)$_2$/ligand/photocatalyst in HFIP solvent can perform meta-acetoxylation under a household compact fluorescent lamp (CFL) bulb (see Supporting Information, Section 3). It was worth noting that the internal temperature of the reaction was found to lie between 30 and 35 °C throughout the reaction time.

With the suitable reaction conditions, the protocol was subsequently explored to generalize the scope of the transformation concerning arene substrates (Scheme 2). In

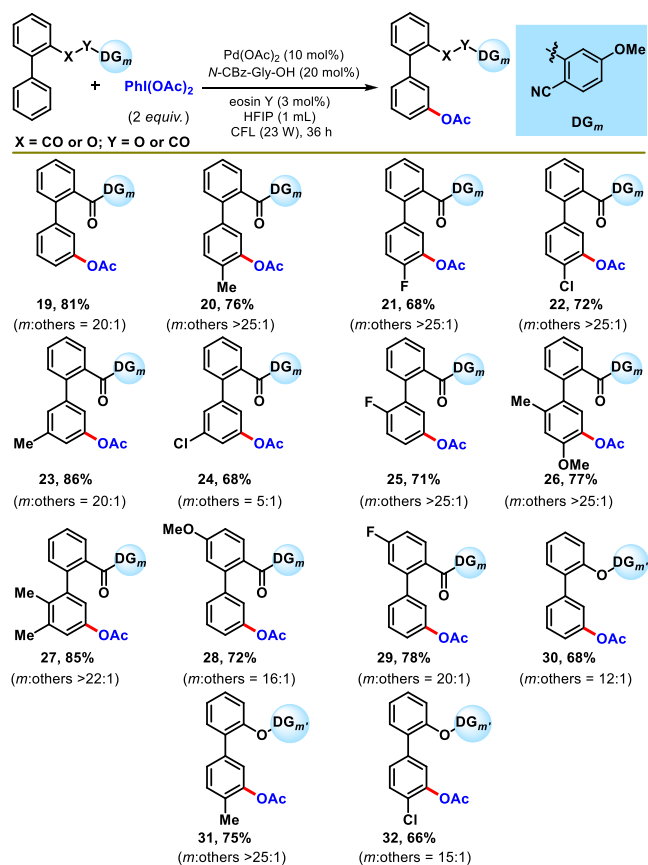**Scheme 2. Scope of the Reaction with Phenylacetic Acid Derivatives**[a]
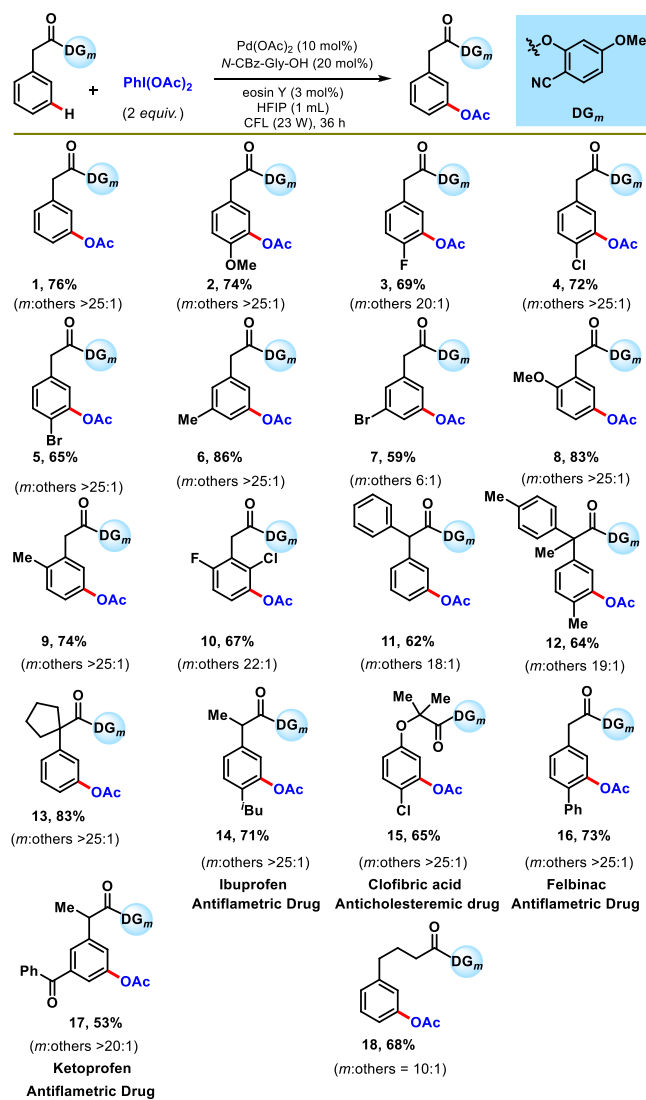
general, phenylacetic acid derivatives with different substitution patterns underwent meta-acetoxylation smoothly, affording products in moderate-to-good yield with excellent selectivity (53−86%). Substitution of an electronically differentiated group at the para-position does not hamper the selectivity, although a moderate yield was observed for the electron-withdrawing group (2−5) (Scheme 2). The presence of a methyl group at the meta-position of phenylacetic acid (6) delivered the highest yield and selectivity (86%, >25:1). Furthermore, ortho-substituted phenylacetic acid produced synthetically useful yield and selectivity (8−10) (Scheme 2). Diphenylacetic acids (11 and 12) were also working well under optimized conditions, affording meta-acetoxylated products in good yield and exclusive selectivity (Scheme 2). Tethering of a cyclopentyl group at the α-position of phenylacetic acid (13) was also well tolerated. Inspired by the versatility of the protocol, we desired to expand the protocol for the late-stage functionalization of marketed drugs and agrochemicals (Scheme 2). To this aim, ibuprofen (14), clofibric acid (15), felbinac (16), and ketoprofen (17) were transformed to their meta-acetoxylated derivatives in good yield and selectivity. Increasing the chain length of the directing template decreased the meta-selectivity of the protocol, as evident from the outcome of 4-phenylbutanoic acid (18).

To further diversify the structural motifs which are yet to be utilized for the meta-acetoxylation reaction, biphenyl carboxylic acid and alcohols were tested under the optimized reaction conditions (Scheme 3). It was worth noting that biphenyl carboxylic acid showed similar reactivity as phenylacetic acid, affording meta-acetoxylated products with good yield and selectivity (19−29) (Scheme 3). The positional biases of the substituents resulted in a similar reactivity pattern as phenylacetic acid. Additionally, the incorporation of a functional group at the arene ring tethering directing template (28 and 29) also delivered synthetically acceptable yield and selectivity. Furthermore, biphenyl alcohols were also found as suitable substrates for photoinduced meta-acetoxylation using 2-carboxy benzonitrile as an effective directing template (Scheme 3). Biphenyl alcohols (30−32) matched biphenyl carboxylic acids, affording meta-acetoxylated products in good yield (66−75%), except for a slightly lesser selectivity for unsubstituted (30) and para-chloro (32) substrates. After the successful photoinduced meta-acetoxylation of ester-linked arenes, we turned our focus to check the feasibility of the protocol for the sulfonyl-linked benzyl arenes (Scheme 4). This will clearly set a platform to compare the thermal and photochemical modes of reaction. The results obtained for the various substituted sulfonyl-linked substrates (entries 33−46) were satisfying and gave useful yields of the expected products with excellent selectivity. A range of electron-donating and electron-withdrawing substituents were compatible, irrespective of their position in the arene. It is important to mention that the present photoredox condition delivered superior selectivity for these classes of substrates over the thermal-mediated C−H acetoxylation reaction. Furthermore, the robustness of the protocol was demonstrated by the meta-acetoxylation reaction of the phosphonyl-tethered arenes (47 and 48) (Scheme 4).
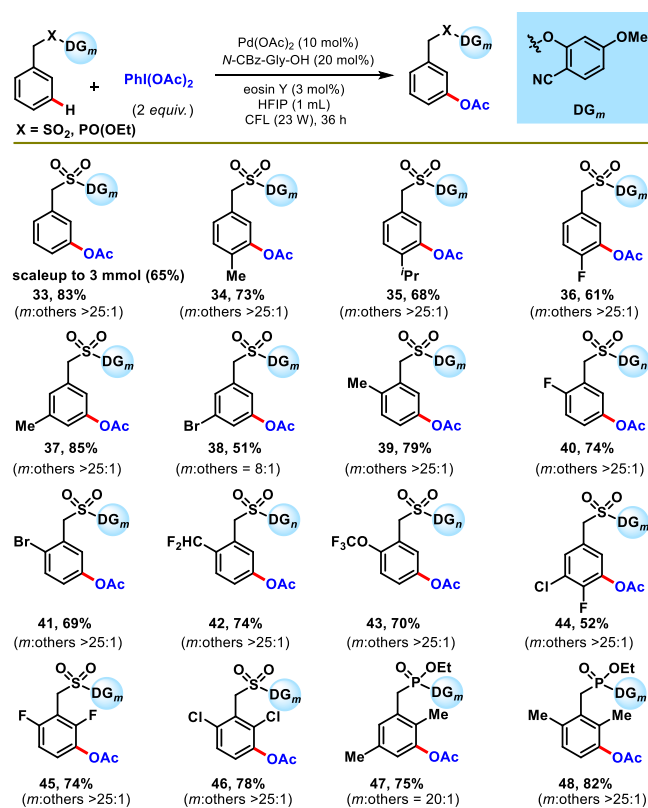
In order to check the feasibility of other acetoxylating sources, PhI(TFA)$_2$ was used, and it led to the formation of the meta-hydroxylated compound as the only product (Scheme 5). The formation of hydroxylated products can be rationalized due to the higher electrophilicity of trifluoroacetate ester

[a]Reaction conditions: substrate (1 equiv), PhI(OAc)$_2$ (2 equiv), Pd(OAc)$_2$ (10 mol %), N-Cbz-Gly-OH (20 mol %), eosin Y (3 mol %), HFIP (1 mL), CFL (23 W), 30−35 °C, 36 h. Isolated yields are reported.

Scheme 3. Scope of the Reaction with Biphenyl Acid/Alcohol Derivatives[a]

19, 81%
(*m*:others = 20:1)

20, 76%
(*m*:others >25:1)

21, 68%
(*m*:others >25:1)

22, 72%
(*m*:others >25:1)

23, 86%
(*m*:others = 20:1)

24, 68%
(*m*:others = 5:1)

25, 71%
(*m*:others >25:1)

26, 77%
(*m*:others >25:1)

27, 85%
(*m*:others >22:1)

28, 72%
(*m*:others = 16:1)

29, 78%
(*m*:others = 20:1)

30, 68%
(*m*:others = 12:1)

31, 75%
(*m*:others >25:1)

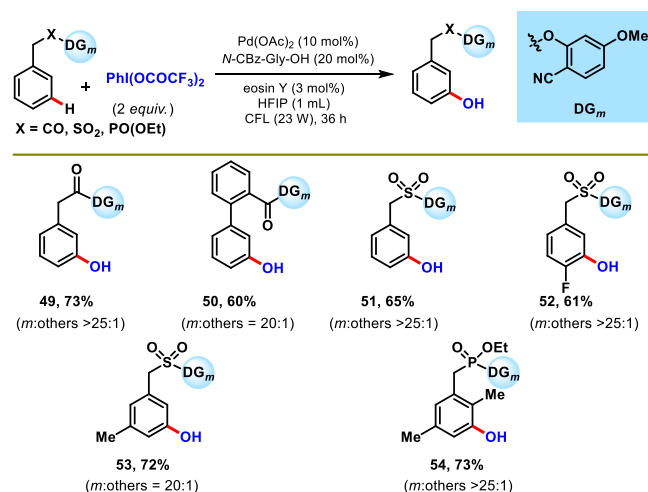**32**, 66%
(*m*:others = 15:1)

[a]Reaction conditions: substrate (1 equiv), PhI(OAc)$_2$ (2 equiv), Pd(OAc)$_2$ (10 mol %), N-Cbz-Gly-OH (20 mol %), eosin Y (3 mol %), HFIP (1 mL), CFL (23 W), 30−35 °C, 36 h. Isolated yields are reported. DG$^{m'}$ = 2-carboxy benzonitrile.

carbonyl, which is likely hydrolyzed in situ. This observation was further confirmed experimentally, where an independently synthesized trifluoro-acetoxylated substrate afforded the hydroxylated product quantitatively when treated under standard reaction conditions (see Supporting Information, Section 5). A similar reactivity trend for *meta*-hydroxylation was observed as for *meta*-acetoxylation (entries 49−54), and it was demonstrated through representative examples of various arenes (Scheme 5). The present photoinduced protocol could also be scaled up (3 mmol) without altering the selectivity and affording the *meta*-acetoxylation product in acceptable yield (**33**, see Supporting Information, Section 4.F.).

Under thermal conditions, the Pd-catalyzed C(*sp*^{2})-H-acetoxylation reaction followed a Pd^{II}/Pd^{IV} catalytic cycle[12−25] in contrast to photoredox catalysis, where two catalytic cycles operate synergistically. The merger of photocatalysis with Pd catalysis can reroute the traditional Pd-catalyzed reactions, thereby enabling the reaction development through an entirely new mechanistic paradigm. To delve into the possible reaction mechanism for this photoinduced Pd-catalyzed *meta*-acetoxylation reaction, a series of experiments were conducted. As discussed earlier, in the absence of light (dark condition) and a photocatalyst (eosin Y), no desired product formation was observed highlighting the role of light and the photocatalyst in the transformation. In our previous report, we demonstrated that light plays a significant role in the

Scheme 4. Scope of the Reaction with Sulfonyl- and Phosphonate-Linked Arenes[a]

33, scaleup to 3 mmol (65%)
(*m*:others >25:1)

34, 73%
(*m*:others >25:1)

35, 68%
(*m*:others >25:1)

36, 61%
(*m*:others >25:1)

37, 85%
(*m*:others >25:1)

38, 51%
(*m*:others = 8:1)

39, 79%
(*m*:others >25:1)

40, 74%
(*m*:others >25:1)

41, 69%
(*m*:others >25:1)

42, 74%
(*m*:others >25:1)

43, 70%
(*m*:others >25:1)

44, 52%
(*m*:others >25:1)

45, 74%
(*m*:others >25:1)

46, 78%
(*m*:others >25:1)

47, 75%
(*m*:others = 20:1)

48, 82%
(*m*:others >25:1)

[a]Reaction conditions: substrate (1 equiv), PhI(OAc)$_2$ (2 equiv), Pd(OAc)$_2$ (10 mol %), N-Cbz-Gly-OH (20 mol %), eosin Y (3 mol %), HFIP (1 mL), CFL (23 W), 30−35 °C, 36 h. Isolated yields are reported.

Scheme 5. Representative Examples for *meta*-Hydroxylation of Various Arenes[a]

49, 73%
(*m*:others >25:1)

50, 60%
(*m*:others = 20:1)

51, 65%
(*m*:others >25:1)

52, 61%
(*m*:others >25:1)

53, 72%
(*m*:others = 20:1)

54, 73%
(*m*:others >25:1)

[a]Reaction conditions: substrate (1 equiv), PhI(CO$_2$CF$_3$)$_2$ (2 equiv), Pd(OAc)$_2$ (10 mol %), N-Cbz-Gly-OH (20 mol %), eosin Y (3 mol %), HFIP (1 mL), CFL (23 W), 30−35 °C, 36 h. Isolated yields are reported.

C−H activation process. To further confirm the hypothesis, when a model reaction was set up in the absence of PhI(OAc)$_2$, a homo-dimerized product was obtained through

Scheme 6. Understanding the Mechanism for Pd-Catalyzed Photoredox *meta*-Acetoxylation of Arenes[a]
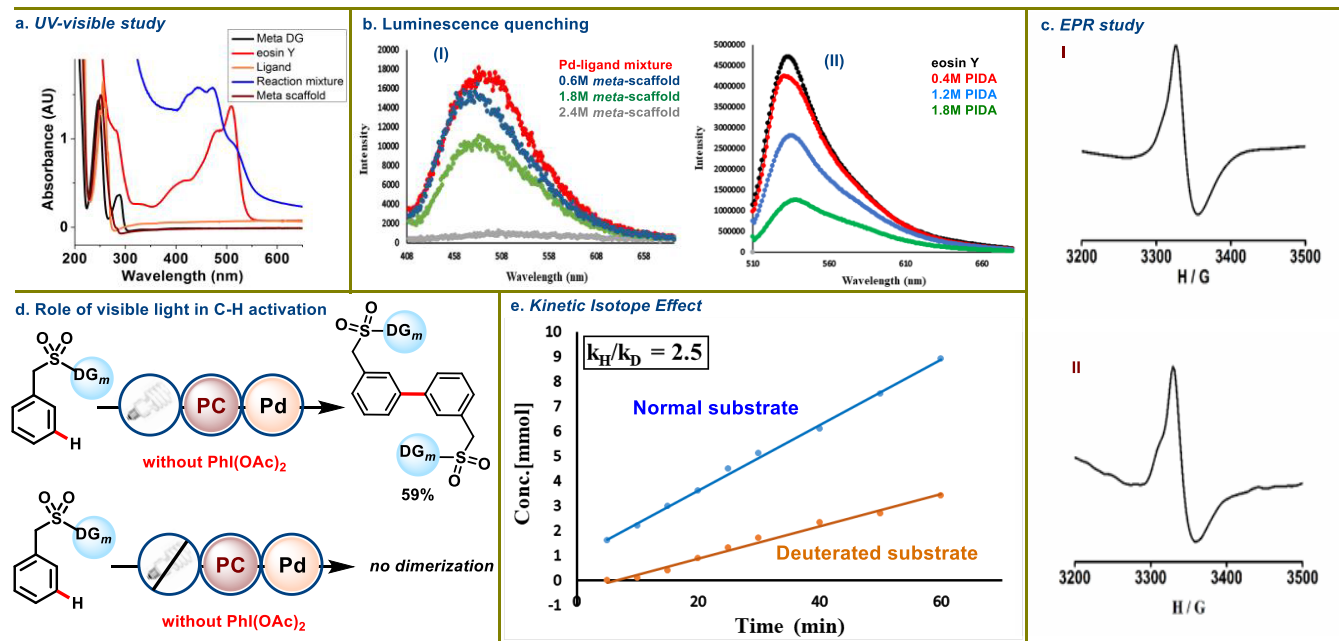
[a]Mechanistic investigations: (a) UV−vis absorption spectroscopy studies of the reaction components and reaction mixture. (b) Luminescence quenching experiments. (c) EPR spectroscopy for the detection of radical species. (I) eosin Y, PhI(OAc)$_2$ in HFIP at 100 K (g = 1.993), (II) scaffold, ligand, Pd(OAc)$_2$, eosin Y, PhI(OAc)$_2$ in HFIP at 100 K (g = 2.001). (d) Role of visible light in C−H activation. (e) Kinetic isotope effect studies.

cross-dehydrogenative coupling engaging the *meta*-C−H bond, which remains unreactive at room temperature in dark conditions (Scheme 6d). The requirement of light irradiation for dimerization indicates that the threshold energy required for the C−H activation step is fulfilled by photons. Apart from this, the conversion profile of the reaction was supervised through on/off experiments (see Supporting Information, Section 6.V.). The *meta*-acetoxylated product formation ceased when the CFL was switched off, signifying the requirement of constant photoirradiation for an effective outcome. A UV− visible study of individual reaction components and reaction mixture was carried out, and a broad signal between 440 and 480 nm for the reaction mixture that falls in the visible region is expected to be the light-absorbing species to favor the C−H activation step (Scheme 6a). The role of light in the C−H activation step is the key feature of this protocol. In order to understand the photomediated C−H activation via the intermediate **C** to **D**, luminescence quenching (Scheme 6b) experiment was performed. Initially, we have taken the palladium catalyst and the *meta*-scaffold, but the emission profile suggests that there is no emission spectra for the palladium catalyst. Hence, the luminescence quenching experiment between the Pd catalyst and the scaffold cannot be performed. This further strengthens our hypothesis that the overall complex of the ligand, Pd catalyst, and *meta*-scaffold undergoes C−H activation in the presence of visible light. Therefore, we have performed another experiment, where an equimolar mixture of the Pd catalyst−ligand was taken and quenching experiment was performed in the presence of the *meta*-scaffold. Interestingly, we observed the quenching phenomenon for the Pd catalyst and ligand mixture (Scheme 6b, I). This observation further corroborated with our hypothesis that light is compulsory and has an integral role in the C−H activation step. Additionally, we have performed

the quenching experiment for the photocatalyst and PhI-(OAc)$_2$. The result fits with our mechanistic postulate as the interaction of the photocatalyst and PhI(OAc)$_2$ was observed by the quenching experiment (Scheme 6b, II). To understand the nature of the reaction mechanism, radical quenching experiments were performed with 3 equiv of 2,2,6,6-tetramethylpiperidin-1-oxyl (TEMPO), phenyl *N*-tert-butylnitrone (PNB), and butylated hydroxytoluene (BHT), respectively (see Supporting Information, Section 6.VIII.). A omplete inhibition of the product formation suggests the generation of radical species in the reaction. The photo-irradiated generation of radical species from PhI(OAc)$_2$ is documented in the literature;[79−81] however, the intriguing aspect of the protocol is how the Pd substrate cooperativity enables the *meta*-oxygenation of arenes by engaging the in situ-generated acetoxy radical. In order to gain an insight into the aforesaid aspect, EPR study of the eosin Y and PhI(OAc)$_2$ mixture under light at different time intervals was conducted and was found to be active. On the contrary, in the absence of either eosin Y or light, it was found to be EPR-silent, amplifying their role in the generation of acetoxy radicals. Furthermore, a prominent EPR signal was also observed for the standard reaction, indicating the formation of a radical species in the reaction medium (Scheme 6c). Also, quantitative iodobenzene formation was observed when an equimolar mixture of eosin Y and PhI(OAc)$_2$ was irradiated with light for 6 h (see Supporting Information, Section 6.VI.). To get further insights into the complexity of the reaction mechanism, the coordination affinity of Pd with the ligand and substrate was monitored through ^{1}H NMR. It was observed that the acetic acid (-CH$_3$) peak intensified when the substrate was added to the stoichiometric Pd(OAc)$_2$−ligand mixture (see Supporting Information, Section 10.A.). The phenomenon of the photo-induced C−H palladation step was also monitored through the
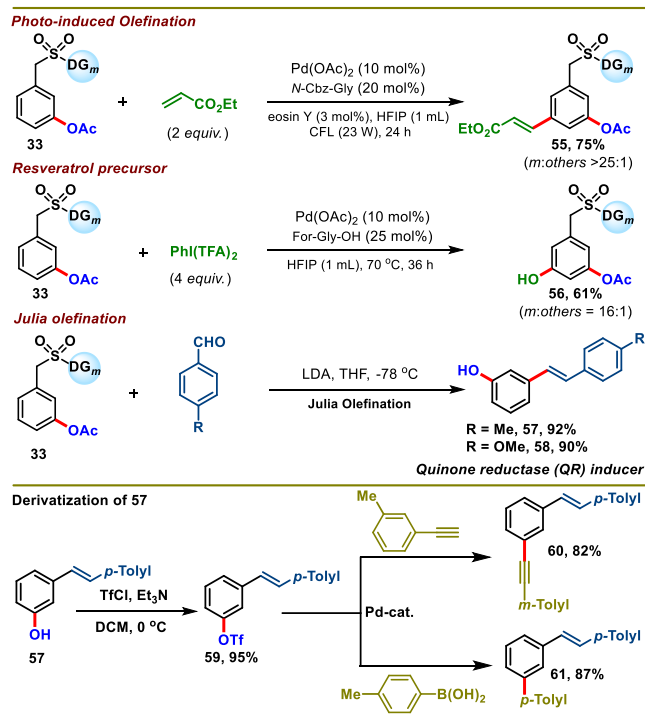
Scheme 7. Plausible Mechanism for *meta*-Acetoxylation of Arenes
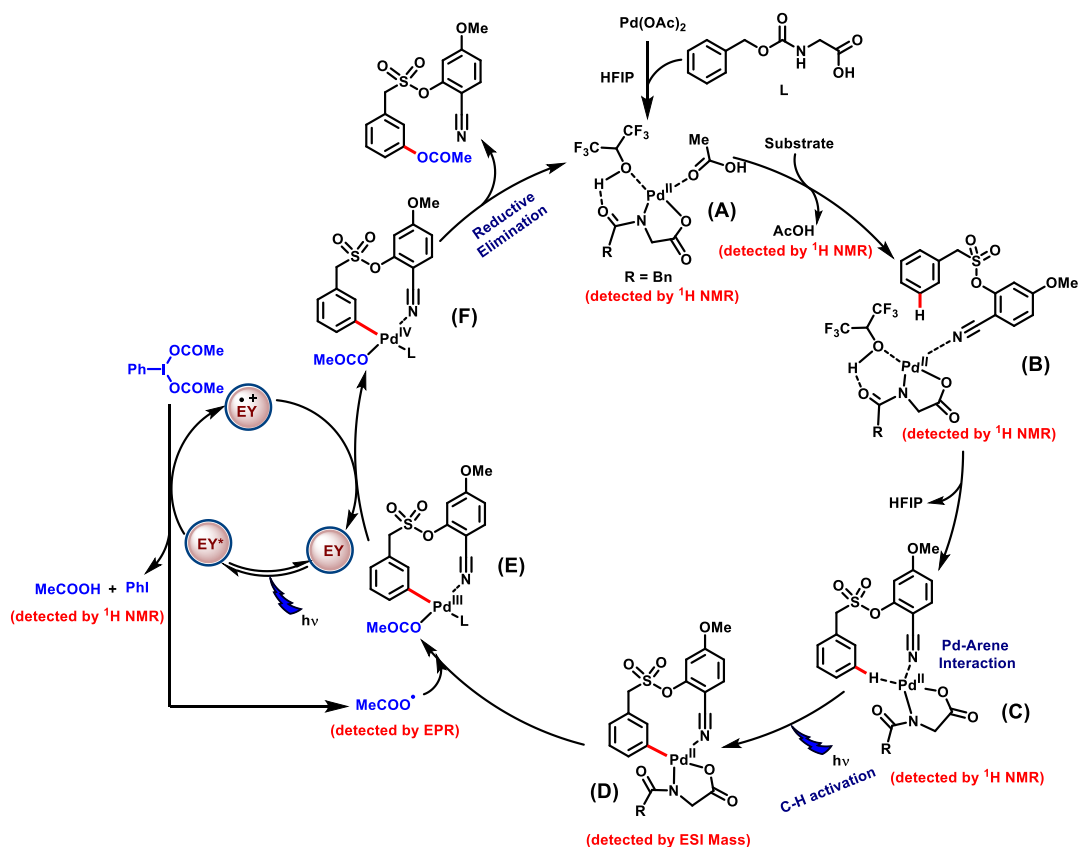
¹H NMR of reaction mixtures at room temperature in dark and under visible light. When the reaction mixture was kept under dark conditions, no shift in the peak of the ¹H NMR signal was observed, while the reaction kept under visible light showed a significant shift in signal (see Supporting Information, Section 10.B.). This observation further strengthens our hypothesis on the role of visible light in the C–H activation step. The presence of the C–H-palladated intermediate was also supported by the ESI-MS studies of the reaction mixture in the absence of PhI(OAc)$_2$, while in dark condition, no C–H-activated complex mass was observed (see Supporting Information, Section 10.C.). All these observations further strengthen the hypothesis on the role of visible light in the C–H activation step. The isotope-labeling experiment carried out between nondeuterated and deuterated substrates showed a high value of the kinetic isotope effect ($k_H/k_D = 2.5$) (see Supporting Information, Section 7) (Scheme 6e). The high value of KIE explicitly establishes that the C–H activation step is likely to be the rate-limiting step in the overall transformation. Furthermore, the kinetic study showed the first-order rate dependency for the substrate, ligand, and palladium catalyst, confirming their participation in the rate-limiting step (see Supporting Information, Section 8). Relying on these observations and literature precedence, an intuitive mechanistic cycle is proposed involving Pd^{II}/Pd^{III}/Pd^{IV} intermediates (Scheme 7). The weak coordination of palladium with the nitrile group brings the Pd–ligand complex in close proximity to the *meta*-C–H bond, which activates the C–H bond through photoexcitation to form a large palladacyclic intermediate **D**. Next, the acetoxy radical formed through eosin Y-assisted reduction of PhI(OAc)$_2$ coordinates with

intermediate **D** to afford the Pd^{III} intermediate **E** (Scheme 7). One electron oxidation of intermediate **E** by oxidized eosin Y results in the regeneration of eosin Y and Pd^{IV} intermediate **F**, which undergoes reductive elimination to deliver the *meta*-acetoxylated product and restore the Pd^{II} catalyst.

The *meta*-acetoxylated product (**33**) was utilized for further functionalization to deliver synthetically versatile compounds (Scheme 8). The olefination reaction of *meta*-acetoxylated product delivered the *meta*-selective olefinated compound (**55**) in good yield (75%) and excellent selectivity. Similarly, *meta*-selective hydroxylation of the product (**33**) resulted in the formation of a potential resveratrol precursor (**56**) in moderate yield and excellent selectivity. Furthermore, the sulfonyl linker of the benzylsulfonyl ester scaffold can be easily cleaved through modified Julia olefination conditions (Scheme 8). When *meta*-acetoxylated products reacted with aldehydes under modified Julia olefination conditions, *meta*-hydroxylated alkenes (**57** and **58**) with a phase II "quinone reductase" (QR) activity inducer (**58**) were obtained in good yields. Subsequently, the isolated *meta*-hydroxylated alkene (**57**) was easily masked with triflate (**59**), which was then transformed into synthetically useful molecules via alkynylation (**60**) and arylation (**61**) reactions (Scheme 8).

In summary, using the synergistic merger of photocatalysis and Pd catalysis, we have developed a highly efficient and selective photoinduced *meta*-oxygenation of a variety of arene systems. The reaction features a high level of regioselectivity at ambient temperature and is compatible for a series of functional groups. In the present protocol, light energy is involved in C–H activation as well as acetoxy radical generation. The control experiments suggest the formation of

Scheme 8. Application of the *meta*-Acetoxylated Product

Photo-induced Olefination

Resveratrol precursor

Julia olefination

Derivatization of 57

radical species in the reaction and the involvement of Pd^{II}/Pd^{III}/Pd^{IV} species in the catalytic cycle. The significance of the present transformation has been illustrated through the synthesis of the resveratrol precursor and the phase II QR activity inducer.

■ METHODS

General Procedure for *meta*-Acetoxylation of Phenylacetic Acid Derivatives

In an oven-dried screw-capped reaction tube charged with a magnetic stir bar, the corresponding ester of phenyl acetic acid (0.1 mmol), Pd(OAc)$_2$ (10 mol %), N-Cbz-Gly-OH (20 mol %), eosin Y (3 mol %), and PhI(OAc)$_2$ (0.2 mmol, 2 equiv) in 1 mL of 1,1,1,3,3,3-hexafluoro-2-propanol (HFIP) were added. The reaction tube was capped and placed 3 cm away from four 23 W household CFL bulbs under stirring (1500 rpm) at room temperature for 36 h. The temperature was maintained at approximately 30−35 °C through cooling with a fan. Upon completion, the mixture was diluted with ethyl acetate and filtered through a celite pad. The filtrate was evaporated under reduced pressure, and the crude mixture was purified by column chromatography using silica (100−200 mesh size) and petroleum ether/ethyl acetate as the eluent.

General Procedure for *meta*-Acetoxylation of Biphenyl Ester/Alcohol Derivatives

In an oven-dried screw-capped reaction tube charged with a magnetic stir bar, the corresponding biphenyl ester/alcohol (0.1 mmol), Pd(OAc)$_2$ (10 mol %), N-Cbz-Gly-OH (20 mol %), eosin Y (3 mol %), and PhI(OAc)$_2$ (0.2 mmol, 2 equiv) in 1 mL of 1,1,1,3,3,3-hexafluoro-2-propanol (HFIP) were added. The reaction tube was capped and placed 3 cm away from four 23 W household CFL bulbs under stirring (1500 rpm) at room temperature for 36 h. The temperature was maintained at approximately 30−35 °C through cooling with a fan. Upon completion, the mixture was diluted with ethyl acetate and filtered through a celite pad. The filtrate was evaporated under reduced pressure, and the crude mixture was purified by column chromatography using silica (100−200 mesh size) and petroleum ether/ethyl acetate as the eluent.

General Procedure for *meta*-Acetoxylation of Sulfonyl/Phosphonyl Ester Derivatives

In an oven-dried screw-capped reaction tube charged with a magnetic stir bar, the corresponding sulfonyl/phosphonyl ester (0.1 mmol), Pd(OAc)$_2$ (10 mol %), N-Cbz-Gly-OH (20 mol %), eosin Y (3 mol %), and PhI(OAc)$_2$ (0.2 mmol, 2 equiv) in 1 mL of 1,1,1,3,3,3-hexafluoro-2-propanol (HFIP) were added. The reaction tube was capped and placed 3 cm away from four 23 W household CFL bulbs under stirring (1500 rpm) at room temperature for 36 h. The temperature was maintained at approximately 30−35 °C through cooling with a fan. Upon completion, the mixture was diluted with ethyl acetate and filtered through a celite pad. The filtrate was evaporated under reduced pressure, and the crude mixture was purified by column chromatography using silica (100−200 mesh size) and petroleum ether/ethyl acetate as the eluent.

General Procedure for *meta*-Hydroxylation of Various Arene Derivatives

In an oven-dried screw-capped reaction tube charged with a magnetic stir bar, the corresponding sulfonyl/phosphonyl ester (0.1 mmol), Pd(OAc)$_2$ (10 mol %), N-Cbz-Gly-OH (20 mol %), eosin Y (3 mol %), and PhI(OCOCF$_3$)$_2$ (0.2 mmol, 2 equiv) in 1 mL of 1,1,1,3,3,3-hexafluoro-2-propanol (HFIP) were added. The reaction tube was capped and placed 3 cm away from four 23 W household CFL bulbs under stirring (1500 rpm) at room temperature for 36 h. The temperature was maintained at approximately 30−35 °C through cooling with a fan. Upon completion, the mixture was diluted with ethyl acetate and filtered through a celite pad. The filtrate was evaporated under reduced pressure, and the crude mixture was purified by column chromatography using silica (100−200 mesh size) and petroleum ether/ethyl acetate as the eluent.

General Procedure for *meta*−*meta* Homocoupling

In an oven-dried screw-capped reaction tube charged with a magnetic stir bar, the corresponding sulfonic ester (0.1 mmol), Pd(OAc)$_2$ (10 mol %), N-CBz-Gly-OH (20 mol %), and eosin Y (3 mol %) in 1 mL of 1,1,1,3,3,3-hexafluoro-2-propanol (HFIP) were added. The reaction tube was capped and placed 3 cm away from four 23 W household CFL bulbs under stirring (1500 rpm) at room temperature for 36 h. The temperature was maintained at approximately 30−35 °C through cooling with a fan. Upon completion, the mixture was diluted with ethyl acetate and filtered through a celite pad. The filtrate was evaporated under reduced pressure, and the yield was monitored using the ^{1}H NMR signal in the presence of 1,3,5-trimethoxybenzene as the internal standard.

General Procedure for Scale-Up Reaction

In an oven-dried screw-capped reaction tube charged with a magnetic stir bar, the corresponding sulfonyl ester (3.0 mmol), Pd(OAc)$_2$ (10 mol %), N-Cbz-Gly-OH (20 mol %), eosin Y (3 mol %), and PhI(OAc)$_2$ (6.0 mmol, 2 equiv) in 10 mL of 1,1,1,3,3,3-hexafluoro-2-propanol (HFIP) were added. The reaction tube was capped and placed 3 cm away from four 23 W household CFL bulbs under stirring (1500 rpm) at room temperature for 36 h. The temperature was maintained at approximately 30−35 °C through cooling with a fan. Upon completion, the mixture was diluted with ethyl acetate and filtered through a celite pad. The filtrate was evaporated under reduced pressure, and the crude mixture was purified by column chromatography using silica (100−200 mesh size) and petroleum ether/ethyl acetate as the eluent.

■ ASSOCIATED CONTENT

Ⓢ Supporting Information

The Supporting Information is available free of charge at https://pubs.acs.org/doi/10.1021/jacsau.3c00231.

> Experimental details including starting material synthesis, optimization details, mechanistic study, characterization data, and ^{1}H and ^{13}C NMR spectra of all the isolated compounds (PDF)

■ AUTHOR INFORMATION

Corresponding Authors

Haibo Ge − *Department of Chemistry and Biochemistry, Texas Tech University, Lubbock, Texas 79409-1061, United States;* ⊙ orcid.org/0000-0001-6727-4602; Email: haibo.ge@ttu.edu

Debabrata Maiti − *Department of Chemistry, Indian Institute of Technology Bombay, Powai, Mumbai 400076, India;* ⊙ orcid.org/0000-0001-8353-1306; Email: dmaiti@iitb.ac.in

Authors

Wajid Ali − *Department of Chemistry, Indian Institute of Technology Bombay, Powai, Mumbai 400076, India*

Argha Saha − *Department of Chemistry, Indian Institute of Technology Bombay, Powai, Mumbai 400076, India*

Complete contact information is available at:
https://pubs.acs.org/10.1021/jacsau.3c00231

Author Contributions

[⊥]W.A. and A.S. contributed equally

Author Contributions

The manuscript was written through the contributions of all authors. All authors have given approval to the final version of the manuscript. W.A. and A.S. contributed equally.

Notes

The authors declare no competing financial interest.

■ ACKNOWLEDGMENTS

■ REFERENCES

(1) McMurray, L.; O'Hara, F.; Gaunt, M. J. Recent developments in natural product synthesis using metal-catalysed C−H bond functionalization. *Chem. Soc. Rev.* **2011**, *40*, 1885−1898.

(2) Abrams, D. J.; Provencher, P. A.; Sorensen, E. J. Recent applications of C−H functionalization in complex natural product synthesis. *Chem. Soc. Rev.* **2018**, *47*, 8925−8967.

(3) Liu, Y.; Ge, H. Site-selective C−H arylation of primary aliphatic amines enabled by a catalytic transient directing group. *Nat. Chem.* **2017**, *9*, 26−32.

(4) Wencel-Delord, J.; Glorius, F. C−H bond activation enables the rapid construction and late-stage diversification of functional molecules. *Nat. Chem.* **2013**, *5*, 369−375.

(5) Cernak, T.; Dykstra, K. D.; Tyagarajan, S.; Vachal, P.; Krska, S. W. The medicinal chemist's toolbox for late-stage functionalization of drug-like molecules. *Chem. Soc. Rev.* **2016**, *45*, 546−576.

(6) Patterson, L. D.; Miller, M. J. Enzymatic deprotection of the cephalosporin 3′-acetoxy group using candida antarctica Lipase B. *J. Org. Chem.* **2010**, *75*, 1289−1292.

(7) Fuerst, E. P.; Arntzen, C. J.; Pfister, K.; Penner, D. Herbicide cross-resistance in triazine-resistant biotypes of four species. *Weed Sci.* **1986**, *34*, 344−353.

(8) May, J. A.; Ratan, H.; Glenn, J. R.; Losche, W.; Spangenberg, P.; Heptinstall, S. GPIIb-IIIa antagonists cause rapid disaggregation of platelets pre-treated with cytochalasin D. Evidence that the stability of platelet aggregates depends on normal cytoskeletal assembly. *Platelets* **1998**, *9*, 227−232.

(9) O'Connor, S. E.; Grosset, A. The pharmacological basis and pathophysiological significance of the heart rate-lowering property of diltiazem. *Fundam. Clin. Pharmacol.* **1999**, *13*, 145−153.

(10) Zhang, B.; Guo, R.; Hu, Y.; Dong, X.; Lin, N.; Dai, X.; Wu, H.; Ma, S.; Yang, B. Design, synthesis and biological evaluation of valepotriate derivatives as novel antitumor agents. *RSC Adv.* **2017**, *7*, 31899.

(11) Murakami, A.; Kitazono, Y.; Jiwajinda, S.; Koshimizu, K.; Ohigashi, H. Niaziminin, a thiocarbamate from the leaves of Moringa oleifera, holds a strict structural requirement for inhibition of tumor-promoter-induced Epstein-Barr virus activation. *Planta Med.* **1998**, *64*, 319−323.

(12) Lyons, T. W.; Sanford, M. S. Palladium-catalyzed ligand-directed C−H functionalization reactions. *Chem. Rev.* **2010**, *110*, 1147−1169.

(13) Dick, A. R.; Hull, K. R.; Sanford, M. S. A highly selective catalytic method for the oxidative functionalization of C-H bonds. *J. Am. Chem. Soc.* **2004**, *126*, 2300−2301.

(14) Yadav, M. R.; Rit, R. K.; Sahoo, A. K. Sulfoximines: A reusable directing group for chemo- and regioselective ortho C−H oxidation of arenes. *Chem. − Eur. J.* **2012**, *18*, 5541−5545.

(15) Zhang, Q.; Wang, Y.; Yang, T.; Li, L.; Li, D. Palladium catalyzed *ortho*-C−H-benzoxylation of 2-arylpyridines using iodobenzene dibenzoates. *Tetrahedron Lett.* **2015**, *56*, 6136−6141.

(16) Chen, K.; Wang, D.; Li, Z.-W.; Liu, Z.; Pan, F.; Zhang, Y.-F.; Shi, Z.-J. Palladium catalyzed C(*sp*³)−H acetoxylation of aliphatic primary amines to γ-amino alcohol derivatives. *Org. Chem. Front.* **2017**, *4*, 2097−2101.

(17) Li, S.; Cai, L.; Ji, H.; Yang, L.; Li, G. Pd(II)-catalysed *meta*-C−H functionalizations of benzoic acid derivatives. *Nat. Commun.* **2016**, *7*, 10443.

(18) Yang, L.; Fu, L.; Li, G. Incorporation of carbon dioxide into carbamate directing groups: Palladium-catalyzed *meta*-C−H olefination and acetoxylation of aniline derivatives. *Adv. Synth. Catal.* **2017**, *359*, 2235−2240.

(19) Tang, R.-Y.; Li, G.; Yu, J. Q. Conformation-induced remote *meta*-C−H activation of amines. *Nature* **2014**, *507*, 215.

(20) Yang, G.; Lindovska, P.; Zhu, D.; Kim, J.; Wang, P.; Tang, R.-Y.; Movassaghi, M.; Yu, J.-Q. Pd(II)-Catalyzed *meta*-C−H olefination, arylation, and acetoxylation of indolines using a U-shaped template. *J. Am. Chem. Soc.* **2014**, *136*, 10807−10813.

(21) Maji, A.; Bhaskararao, B.; Singha, S.; Sunoj, R. B.; Maiti, D. Directing group assisted *meta*-hydroxylation by C−H activation. *Chem. Sci.* **2016**, *7*, 3147−3153.

(22) Dutta, U.; Modak, A.; Bhaskararao, B.; Bera, M.; Bag, S.; Mondal, A.; Lupton, D. W.; Sunoj, R. B.; Maiti, D. Catalytic arene *meta*-C−H functionalization exploiting a quinoline-based template. *ACS Catal.* **2017**, *7*, 3162−3168.

(23) Bera, M.; Sahoo, S. K.; Maiti, D. Room-temperature *meta*-functionalization: Pd(II)-catalyzed synthesis of 1,3,5-trialkenyl arene and *meta*-hydroxylated olefin. *ACS Catal.* **2016**, *6*, 3575−3579.

(24) Jayarajan, R.; Das, J.; Bag, S.; Chowdhury, R.; Maiti, D. Diverse *meta*-C-H functionalization of arenes across different linker lengths. *Angew. Chem., Int. Ed.* **2018**, *57*, 7659−7663.

(25) Giri, R.; Liang, J.; Lei, J.-G.; Li, J.-J.; Wang, D.-H.; Chen, X.; Naggar, I. C.; Guo, C.; Foxman, B. M.; Yu, J.-Q. Pd-Catalyzed stereoselective oxidation of methyl groups by inexpensive oxidants under mild conditions: A dual role for carboxylic anhydrides in catalytic C-H bond oxidation. *Angew. Chem., Int. Ed.* **2005**, *44*, 7420−7424.

(26) Prier, C. K.; Rankic, D. A.; MacMillan, D. W. C. Visible light photoredox catalysis with transition metal complexes: applications in organic synthesis. *Chem. Rev.* **2013**, *113*, 5322−5363.

(27) Tucker, J. W.; Stephenson, C. R. Shining light on photoredox catalysis: theory and synthetic applications. *J. Org. Chem.* **2012**, *77*, 1617−1622.

(28) Beatty, J. W.; Stephenson, C. R. J. Amine functionalization *via* oxidative photoredox catalysis: methodology development and complex molecule synthesis. *Acc. Chem. Res.* **2015**, *48*, 1474−1484.

(29) Qin, Q.; Jiang, H.; Hu, Z.; Ren, D.; Yu, S. Functionalization of C-H bonds by photoredox catalysis. *Chem. Rec.* **2017**, *17*, 754−774.

(30) Crisenza, G. E. M.; Melchiorre, P. Chemistry glows green with photoredox catalysis. *Nat. Commun.* **2020**, *11*, 803.

(31) Chan, A. Y.; Perry, I. B.; Bissonnette, N. B.; Buksh, B. F.; Edwards, G.; Frye, A. L. I.; Garry, O. L.; Lavagnino, M. N.; Li, Y. B.; Liang, X.; Mao, E.; Millet, A.; Oakley, J. V.; Reed, N. L.; Sakai, H. A.; Seath, C. P.; MacMillan, D. W. C. Metallaphotoredox: The merger of photoredox and transition metal catalysis. *Chem. Rev.* **2022**, *122*, 1485−1542.

(32) Douglas, N. H.; Nicewicz, D. A. Photoredox-catalyzed C−H functionalization reactions. *Chem. Rev.* **2022**, *122*, 1925−2016.

(33) Kärkäs, M. D., Jr.; Porco, J. A.; Stephenson, C. R. J. Photochemical approaches to complex chemotypes: Applications in natural product synthesis. *Chem. Rev.* **2016**, *116*, 9638−9747.

(34) Bach, T.; Hehn, J. P. Photochemical reactions as key Steps in natural product synthesis. *Angew. Chem., Int. Ed.* **2011**, *50*, 1000−1045.

(35) Hoffmann, N. Photochemical reactions as key steps in organic synthesis. *Chem. Rev.* **2008**, *108*, 1052−1103.

(36) Jeong, D. Y.; Lee, D. S.; Lee, H. L.; Nah, S.; Lee, J. Y.; Cho, E. J.; You, Y. Evidence and governing factors of the radical-ion photoredox catalysis. *ACS Catal.* **2022**, *12*, 6047−6059.

(37) Chandrashekar, H. B.; Maji, A.; Halder, G.; Banerjee, S.; Bhattacharyya, S.; Mait, D. Photocatalyzed borylation using water-soluble quantum dots. *Chem. Commun.* **2019**, *55*, 6201−6204.

(38) Ghosh, I.; Marzo, L.; Das, A.; Shaikh, R.; König, B. Visible light mediated photoredox catalytic arylation reactions. *Acc. Chem. Res.* **2016**, *49*, 1566−1577.

(39) Romero, N. A.; Nicewicz, D. A. Organic photoredox catalysis. *Chem. Rev.* **2016**, *116*, 10075−10166.

(40) Shaw, M. H.; Twilton, J.; MacMillan, D. W. C. Photoredox catalysis in organic chemistry. *J. Org. Chem.* **2016**, *81*, 6898−6926.

(41) Noël, T.; Zysman-Colman, E. The promise and pitfalls of photocatalysis for organic synthesis. *Chem Catal.* **2022**, *2*, 468−476.

(42) Govaerts, S.; Nyuchev, A.; Noël, T. Pushing the boundaries of C−H bond functionalization chemistry using flow technology. *J. Flow Chem.* **2020**, *10*, 13−71.

(43) Wei, X.-J.; Abdiaj, I.; Sambiagio, C.; Li, C.; Zysman-Colman, E.; Alcázar, J.; Noël, T. Visible-light-promoted iron-catalyzed C(sp^2)−C(sp^3) Kumada cross-coupling in flow. *Angew. Chem., Int. Ed.* **2019**, *58*, 13030−13034.

(44) Twilton, J.; Le, C. C.; Zhang, P.; Shaw, M. H.; Evans, R. W.; MacMillan, D. W. C. The merger of transition metal and photocatalysis. *Nat. Rev. Chem.* **2017**, *1*, No. 0052.

(45) Buzzetti, L.; Crisenza, G. E. M.; Melchiorre, P. Mechanistic studies in photocatalysis. *Angew. Chem., Int. Ed.* **2019**, *58*, 3730−3747.

(46) Ravelli, D.; Protti, S.; Fagnoni, M. Carbon−Carbon bond forming reactions *via* photogenerated intermediates. *Chem. Rev.* **2016**, *116*, 9850−9913.

(47) Wang, C. S.; Dixneuf, P. H.; Soulé, J. F. Photoredox catalysis for building C-C bonds from C(sp^2)-H bonds. *Chem. Rev.* **2018**, *118*, 7532−7585.

(48) Hopkinson, M. N.; Sahoo, B.; Li, J. L.; Glorius, F. Dual catalysis sees the light: combining photoredox with organo-acid, and transition-metal catalysis. *Chem. − Eur. J.* **2014**, *20*, 3874−3886.

(49) Lipp, A.; Badir, S. O.; Molander, G. Stereoinduction in metallaphotoredox catalysis. *Angew. Chem., Int. Ed.* **2021**, *60*, 1714−1726.

(50) Zhang, H. H.; Chen, H.; Zhu, C.; Yu, S. A review of enantioselective dual transition metal/photoredox catalysis. *Sci. Chi. Chem.* **2020**, *63*, 637.

(51) Shee, M.; Singh, N. D. P. Cooperative photoredox and palladium catalysis: recent advances in various functionalization reactions. *Catal. Sci. Technol.* **2021**, *11*, 742−767.

(52) Cheung, K. P. S.; Sarkar, S.; Gevorgyan, V. Visible light-induced transition metal catalysis. *Chem. Rev.* **2022**, *122*, 1543−1625.

(53) Maiti, S.; Roy, S.; Ghosh, P.; Kasera, A.; Maiti, D. Photo-excited nickel-catalyzed silyl-radical-mediated direct activation of carbamoyl chlorides to access (Hetero)aryl carbamides. *Angew. Chem., Int. Ed.* **2022**, *61*, No. e202207472.

(54) Le, C.; Chen, T. Q.; Liang, T.; Zhang, P.; MacMillan, D. W. C. A radical approach to the copper oxidative addition problem: Trifluoromethylation of bromoarenes. *Science* **2018**, *360*, 1010−1014.

(55) Huang, H.-M.; Bellotti, P.; Erchinger, J. E.; Paulisch, T. O.; Glorius, F. Radical carbonyl umpolung arylation via dual nickel catalysis. *J. Am. Chem. Soc.* **2022**, *144*, 1899−1909.

(56) Guilleard, L.; Wencel-Delord, J. When metal-catalyzed C−H functionalization meets visible-light photocatalysis. *Beilstein J. Org. Chem.* **2020**, *16*, 1754−1804.

(57) Fabry, D. C.; Rueping, M. Merging visible light photoredox catalysis with metal-catalyzed C−H activations: on the role of oxygen and superoxide ions as oxidants. *Acc. Chem. Res.* **2016**, *49*, 1969−1979.

(58) Wang, X.; Xun, X.; Song, H.; Liu, Y.; Wang, Q. Palladium metallaphotoredox-catalyzed 2-arylation of indole derivatives. *Org. Lett.* **2022**, *24*, 4580−4585.

(59) Wang, X.; Yu, M.; Song, H.; Liu, Y.; Wang, Q. Palladium metallaphotoredox-catalyzed 3-acylation of indole derivatives. *Chem. Commun.* **2022**, *58*, 9492−9495.

(60) Lang, S. B.; O'Nele, K. M.; Tunge, J. A. Decarboxylative allylation of amino alkanoic acids and esters via dual catalysis. *J. Am. Chem. Soc.* **2014**, *136*, 13606−13609.

(61) Zoller, J.; Fabry, D. C.; Ronge, M. A.; Rueping, M. Synthesis of indoles using visible light: photoredox catalysis for palladium-catalyzed C-H Activation. *Angew. Chem., Int. Ed.* **2014**, *53*, 13264−13268.

(62) Zhou, C.; Li, P.; Zhu, X.; Wang, L. Merging photoredox with palladium catalysis: Decarboxylative *ortho*-acylation of acetanilides with α-oxocarboxylic acids under mild reaction conditions. *Org. Lett.* **2015**, *17*, 6198−6201.

(63) Song, C.; Zhang, H.-H.; Yu, S. Regio- and enantioselective decarboxylative allylic benzylation enabled by dual palladium/photoredox catalysis. *ACS Catal.* **2022**, *12*, 1428−1432.

(64) Wang, H.; Li, T.; Hu, D.; Tong, X.; Zheng, L.; Xia, C. Acylation of arenes with aldehydes through dual C−H activations by merging photocatalysis and palladium catalysis. *Org. Lett.* **2021**, *23*, 3772−3776.

(65) Narayanam, J. M. R.; Stephenson, C. R. J. Visible light photoredox catalysis: applications in organic synthesis. *Chem. Soc. Rev.* **2011**, *40*, 102−113.

(66) Schultz, D. M.; Yoon, T. P. Solar synthesis: prospects in visible light photocatalysis. *Science* **2014**, *343*, No. 1239176.

(67) Ischay, M. A.; Anzovino, M. E.; Du, J.; Yoon, T. P. Efficient visible light photocatalysis of [2+2] enone cycloadditions. *J. Am. Chem. Soc.* **2008**, *130*, 12886−12887.

(68) Narayanam, J. M. R.; Tucker, J. W.; Stephenson, C. R. J. Electron-transfer photoredox catalysis: Development of a tin-free reductive dehalogenation reaction. *J. Am. Chem. Soc.* **2009**, *131*, 8756−8757.

(69) Parasram, M.; Gevorgyan, V. Visible light-induced transition metal-catalyzed transformations: beyond conventional photosensitizers. *Chem. Soc. Rev.* **2017**, *46*, 6227−6240.

(70) Chuentragool, P.; Kurandina, D.; Gevorgyan, V. Catalysis with palladium complexes photoexcited by visible light. *Angew. Chem., Int. Ed.* **2019**, *58*, 11586−11598.

(71) Kuribara, T.; Nakajima, M.; Nemoto, T. A. A visible-light activated secondary phosphine oxide ligand enabling Pd-catalyzed radical cross-couplings. *Nat. Commun.* **2022**, *13*, 4052.

(72) Zhao, G.; Yao, W.; Mauro, J. N.; Ngai, M.-Y. Excited-state palladium-catalyzed 1,2-spin-center shift enables selective C-2 reduction, deuteration, and iodination of carbohydrates. *J. Am. Chem. Soc.* **2021**, *143*, 1728−1734.

(73) Cheung, K. P. S.; Kurandina, D.; Yata, T.; Gevorgyan, V. Photoinduced palladium-catalyzed carbo-functionalization of conjugated dienes proceeding via radical-polar crossover scenario: 1,2-aminoalkylation and beyond. *J. Am. Chem. Soc.* **2020**, *142*, 9932−9937.

(74) Kvasovs, N.; Iziumchenko, V.; Palchykov, V.; Gevorgyan, V. Visible light-induced Pd-catalyzed alkyl-Heck reaction of oximes. *ACS Catal.* **2021**, *11*, 3749−3754.

(75) Parasram, M.; Chuentragool, P.; Sarkar, D.; Gevorgyan, V. Photoinduced formation of hybrid aryl Pd-radical species capable of 1,5-HAT: Selective catalytic oxidation of silyl ethers into silyl enol ethers. *J. Am. Chem. Soc.* **2016**, *138*, 6340−6343.

(76) Ratushnyy, M.; Parasram, M.; Wang, Y.; Gevorgyan, V. Palladium-catalyzed atom-transfer radical cyclization at remote unactivated C(sp^3)−H Sites: Hydrogen-atom transfer of hybrid vinyl palladium radical intermediates. *Angew. Chem., Int. Ed.* **2018**, *57*, 2712−2715.

(77) Kalyani, D.; McMurtrey, K. B.; Neufeldt, S. R.; Sanford, M. S. Room-temperature C−H arylation: Merger of Pd-catalyzed C−H functionalization and visible-light photocatalysis. *J. Am. Chem. Soc.* **2011**, *133*, 18566−18569.

(78) Saha, A.; Guin, S.; Ali, W.; Bhattacharya, T.; Sasmal, S.; Goswami, N.; Prakash, G.; Sinha, S. K.; Chandrashekar, H. B.; Panda, S.; Anjana, S. S.; Maiti, D. Photoinduced regioselective olefination of arenes at proximal and distal sites. *J. Am. Chem. Soc.* **2022**, *144*, 1929−1940.

(79) He, Z.; Bae, M.; Wu, J.; Jamison, T. F. Synthesis of highly functionalized polycyclic quinoxaline derivatives using visible-light photoredox catalysis. *Angew. Chem., Int. Ed.* **2014**, *53*, 14451−14455.

(80) Xie, J.; Xu, P.; Li, H.; Xue, Q.; Jin, H.; Chenga, Y.; Zhu, C. A room temperature decarboxylation/C−H functionalization cascade by visible-light photoredox catalysis. *Chem. Commun.* **2013**, *49*, 5672−5674.

(81) Paul, A.; Chatterjee, D. R.; Halder, T.; Banerjee, S.; Yadav, S. Metal free visible light photoredox activation of PhI(OAc)$_2$ for the conversion of arylboronic acids to phenols. *Tetrahedron Lett.* **2015**, *56*, 2496−2499.